Available online at www.sciencedirect.com
ScienceDirect
Progress in Natural Science: Materials International 21(2011) 293−300
Progress in Natural Science: Materials International
www.elsevier.com/locate/pnsc

Development of NiTiNb in-situ composite with high damping capacity and high yield strength

Zhen-zhen BAO, Shun GUO, Fu XIAO, Xin-qing ZHAO

School of Materials Science and Engineering, Beihang University, Beijing 100191, China

Received 15 March 2011; accepted 25 July 2011

Abstract: The shape memory alloys are well known to exhibit high damping capacity in martensite state, but possess low yield strength because of the reorientation or de-twining of the martensite variants. The high damping mechanism of shape memory alloys was introduced. The NiTiNb alloys with high yield strength and high damping capacity were designed and prepared. The microstructure evolution, martensitic transformation behavior, damping capacity and mechanical properties of series NiTiNb alloys were investigated. In view of the microstructure characteristics of the NiTiNb in-situ composites, the mechanism associated with high damping capacity and high yield strength was discussed. The results show that NiTiNb alloys feature in in-situ composite, composed of primary NiTi(Nb) phase and fine lamellar eutectics of NiTi(Nb) and β-Nb.

Key words: NiTiNb; shape memory alloy; mechanical properties; damping capacity

1 Introduction

As an important category of functional or smart material, the shape memory alloys have been received increasing attention because of their wide application in various fields, such as aeronautics and astronautics, civil industry and biomedicine [1−2]. It is well known that the shape memory effect and superelasticity of shape memory alloys are attributed to reversible thermoelastic martensitic transformations during cooling/heating treatments or stress loading/downloading process. When the shape memory alloys in martensite state are subjected to external stress, they will response to the stress through a deformation by a so-called de-twining mechanism. By this mechanism, different martensite variations can be transformed to particular one variation that can accommodate the stress induced elongation. By comparison with the martensitic transformation occurred in well known iron based alloys, the carbon steel, for example, the martensite in shape memory alloys is a weak phase and can be easily deformed by de-twining process. By contrast, the austenite phase in shape memory alloys has only one possible orientation and shows relatively strong resistance to external stress, exhibiting higher yield stress than the martensite [2−3]. Owing to the nature of the twin structure of martensite and the coherent interfaces between the martensite variants as well as the martensite/austenite phases, dynamic loading, vibration for example, can be dissipated by the martensite variants reorientation and the de-twining process. This is the reason why the shape memory alloys demonstrate very good damping capacity in the martensite state or in stress induced martensite state.

In recent decades high damping materials have attracted increasing scientific and technological interests, because of their potential applications in a lot of situations, such as reducing noise pollution or mechanical vibration, improving the control precision of machinery and instruments, and protecting buildings against earthquake, etc. It is well known that polymeric materials exhibit very high damping capacity due to their viscous elasticity. However, polymers possess low elastic modulus, which limits the application of this kind of high damping materials for structural purpose. As a matter of fact, in the design of structural damping the merit index is the product of the elastic modulus (stiffness) and the damping coefficient (capacity) [4−5]. According to this principle, several kinds of high damping

Foundation item: Project (50971009) supported by the National Nature Science Foundation of China; Project (2012CB619403) supported by the National Basic Research Program of China; Project (2009ZF51059) supported by the Aviation Science Foundation of China
Corresponding author: Xin-qing ZHAO; Tel: +86-10-82338559; E-mail: xinqing@buaa.edu.cn

metallic materials, called HIDAMETS, have been developed for structural applications. Among these metallic materials, one of the most important alloy families that exhibit high damping property is the shape memory alloys [6].

As a unique representative of shape memory alloys, near equiatomic NiTi alloys with excellent shape memory effect (or superelasticity) and good complex mechanical properties have found wide applications which spans a wide variety of industrial sectors such as aerospace, automotive, biomedical and oil exploration [1]. Besides, research efforts have been extended to employ NiTi shape memory alloys for passive or active control of shock, vibration and noise, because of their high damping property [6−11]. Despite the fact that the NiTi shape memory alloys possess high damping capacity and high ultimate fracture strength, they always perform low yield strength in the martensite state, due to the reorientation and de-twining of martensite variants. For example, binary equi-atomic NiTi alloys always exhibit yield strength from a several tens to 200 MPa [1−2], depending on the composition and temperature. Such low yield strength constructed a limitation to the applications of NiTi shape memory alloys as high damping materials in engineering. Accordingly, it is of technical importance and academic interests to research and develop novel damping alloys with high yield strength and high damping capacity.

In general, high yield strength and good damping capacity are two contradictory aspects for metallic materials. Since the near equiatomic NiTi shape memory alloy does not exhibit high enough yield strength in martensite state, we consider, therefore, the possibility to produce a new kind of high damping in-situ shape memory alloy composites. Such in-situ composites are expected to consist of two structural constituents, one constituent could provide high damping capacity and the other contribute to high yield strength. When the two structural constituents come to a compromise, the composites could possess both good damping capacity and good mechanical properties.

$Ni_{47}Ti_{44}Nb_9$, as a classic shape memory alloy with wide hysteresis and low transformation temperature, has received significant attention because of its convenient installation and transportation during the application in coupling or sealing systems [3,12]. The microstructure of $Ni_{47}Ti_{44}Nb_9$ is characterized by a in-situ composite feature, i.e. primary NiTi(Nb) phase as matrix and the eutectics of Nb-rich and NiTi(Nb) phases which embedded in the matrix. Experimental investigations by PIAO [13−14] and by the present authors [15−16] indicated that the microstructure evolution of NiTiNb alloys and the phase transformation temperature are closely dependent on the Ni/Ti ratio and the amount of additive Nb. This suggests that the volume fraction of eutectics and the primary phase as well as the martensitic transformation temperature could be adjusted or tailored by the addition of Nb and the variation mass ratios of Ni to Ti. So, an improvement of mechanical properties can be expected even if NiTi based phase is in martensite state, since large amount of eutectics in the microstructure can effectively resist the yield deformation. In the present paper, NiTiNb shape memory alloys with high yield strength and high damping capacity were reported. The relationships among the mechanical and damping properties, the composition, and the microstructures of NiTiNb shape memory alloys were discussed.

2 Experimental

NiTi and NiTiNb alloys were prepared by induction melting Ti (99.8%, mass fraction), Ni (99.96%) and Nb (99.9%) in water-cooled copper hearth. About ingots 100 g were melted for four times repeatedly and annealed at 850 °C for 24 h for homogenization. And then the ingots were hot rolled at 850 °C into plates of 1 mm in thickness at a reduction rate of 80%. All the samples used for tests and examinations were cut from the plates by a spark electric charge followed by annealing at 850 °C for 1 h and then quenching in ice water. The characteristic phase transformation temperatures were determined by recording the variation of electric resistance with temperature. These characteristic temperatures include martensitic transformation start (M_s) temperature, martensitic transformation finish (M_f) temperature and martensite to austenite transformation start (A_s) temperature. Microstructure observation and quantitative composition analysis of the alloys were performed with a JSM 5600 scanning electron microscope equipped with a energy dispersive X-ray analyzer (Link ISIS−300, Oxford Instruments). X-ray diffraction was carried out with a Regaku D/max 2200pc diffractometer.

Tensile tests were carried out using a MTS−800 mechanical tester. Stress-strain curves were recorded at a strain rate of 1.1×10^{-3} s^{-1} and the temperature of M_s−15 K. Damping tests were performed with a dual cantilever model using a TA Instruments DMA Q800 at frequency of 1 Hz, cooling rate of 3 °C /min and strain amplitude of 1×10^{-4}.

3 Results and discussion

3.1 Microstructure of $(NiTi)_{50-0.5x}Nb_x$ (x=5, 10, 15, 20) alloys

In order to examine the effect of Nb addition on the

microstructure evolution of NiTiNb alloys with a equivalent Ni to Ti ratio, $(NiTi)_{50-0.5x}Nb_x$ series alloys with x of 5, 10, 15, 20, respectively, were prepared. Figure 1 shows the XRD patterns of the as-cast NiTiNb samples.

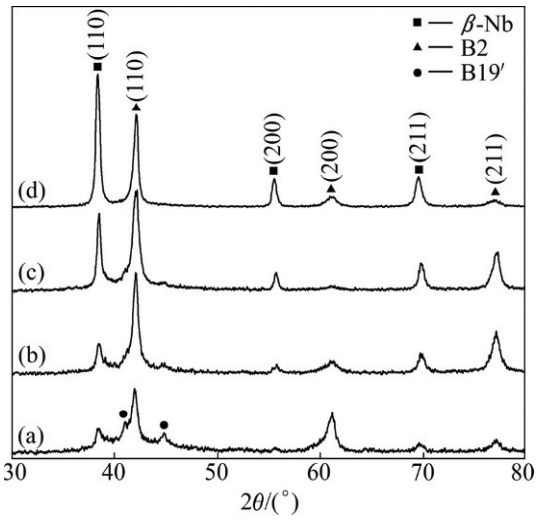

Fig. 1 XRD patterns of as-cast $(NiTi)_{50-0.5x}Nb_x$ alloys: (a) x=5; (b) x=10; (c) x=15; (d) x=20

The XRD patterns in Fig. 1 demonstrate that the constituent phases of $(NiTi)_{50-0.5x}Nb_x$ alloys in as-cast state can be characterized by B2, β-Nb and/or B19′ martensite phases. As expected, the volume fraction of β-Nb phase increases with the increasing Nb addition from 5% to 20% (mole fraction). One can see that the B19′ martensite phase appears in the samples of 5% Nb, 10% Nb and 15% Nb, and that no B19′ martensite phase was observable in the sample of 20% Nb. This means that martensitic transformation took place in the $(NiTi)_{50-0.5x}Nb_x$ alloys with x of 5, 10 and 15 during the cooling from high temperature to room temperature. Referring to the XRD patterns, two diffraction peaks ascribed to B19′ martensite phase, located at 2θ of 41° and 44.9°, weaken gradually from sample (a) to (c). This reveals that the martensite phase volume fraction decreases with the increasing Nb addition, and that the samples with higher Nb addition are of lower M_s temperature. Nevertheless, by comparison with the amount of martensite formed, B2 phase in the alloys of 5% Nb (mole fraction), 10% Nb and 15% Nb is still in a majority of volume fraction. In other words, only partial B2 phase transformed to B19′ martensite at room temperature. It is reasonable to conclude that the M_s temperatures of $(NiTi)_{50-0.5x}Nb_x$ (x=5, 10, 15) alloys are higher than or near to room temperature (25 °C). In some cases with the M_s temperature a little lower than room temperature, a few of martensite could form by stress induced martensitic transformation during the sample preparation.

Figure 2 shows the SEM images of the NiTiNb series alloys. By energy dispersive X-ray spectroscope equipped with the scanning electron microscope, the dark gray regions was recognized to be primary NiTi(Nb) phase which might be B2 phase or a mixture of B2 and B19′ martensite, depending on the Ms temperatures. The bright regions with fine lamellar structure are characterized to be eutectics consisting of NiTi(Nb) and β-Nb phases. The magnification image of the fine lamellar structure of the eutectics is also given in Fig. 2(c)). Obviously, higher Nb content leads to the formation of more volume fraction of eutectic structure when the mole ratio Ti to Ni is kept equivalent. For the samples with 5% Nb and 10% Nb, the NiTi(Nb) phase is in a majority and serves as the matrix on which some eutectic phases distribute randomly. Whereas when the Nb content reaches 15%, the eutectics structure becomes in a majority component and serves as the matrix on which round NiTi(Nb) phase randomly distributes. In particular for the alloy with 20% Nb, the corresponding microstructure is fully composed of fine lamellar eutectics and no isolated NiTi(Nb) phase was observed. These results are in agreement with the research work by PIAO et al [13−14] and the present authors [16].

As shown in Fig. 2, the structures of $(NiTi)_{50-0.5x}Nb_x$ in their as-cast state are not uniform in the microstructure scale, with a exception of $Ti_{40}Ni_{40}Nb_{20}$ which are characterized to be fully fine eutectic structure. As well known, severe deformation could be helpful to homogenize the phase configurations, giving rise to more uniform microstructure. Figure 3 shows the SEM images of as-rolled $Ti_{42.5}Ni_{42.5}Nb_{15}$ and $Ti_{40}Ni_{40}Nb_{20}$ alloys. It is indicated that after the hot rolling at a reduction of 80% in thickness, severe deformation occurred not only in the primary NiTi(Nb) phase but also in the eutectic structure consisting of NiTi(Nb) and β-Nb phases, resulting in more uniform microstructure than as-cast samples. That is, upon a severe hot rolling, nonuniform structure consisting of primary phases and eutectics can be evolved to a eutectic-like structure, i.e. rolling induced eutectics.

3.2 Damping capacity of $(NiTi)_{50-0.5x}Nb_x$ (x=5, 10, 15, 20) alloys

In order to examine the damping capacity of $(NiTi)_{50-0.5x}Nb_x$ alloys, dynamic mechanical analysis was employed to record their internal friction performance, $\tan\delta$, versus the temperature change. Figure 4 represents the damping spectra of as-rolled $(NiTi)_{50-0.5x}Nb_x$ alloys.

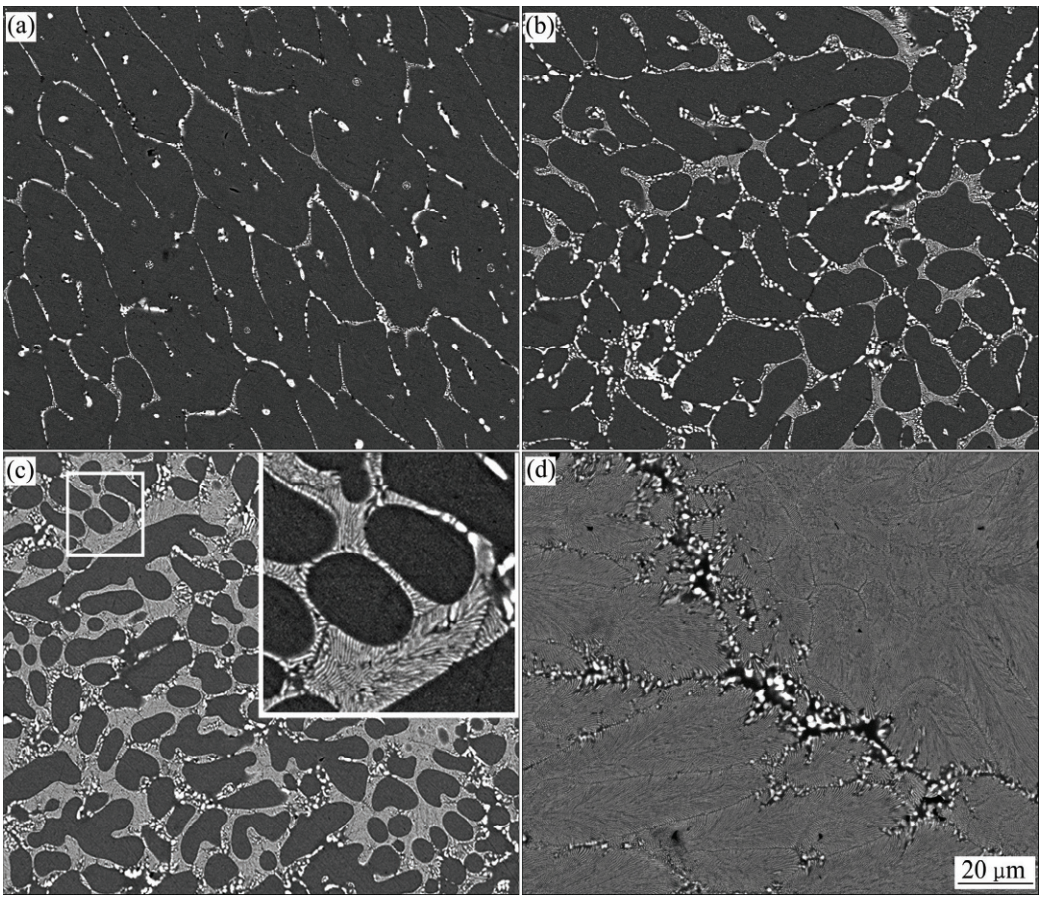

Fig. 2 SEM images of as-cast $(NiTi)_{50-0.5x}Nb_x$ alloys: (a) x=5; (b) x=10; (c) x=15; (d) x=20

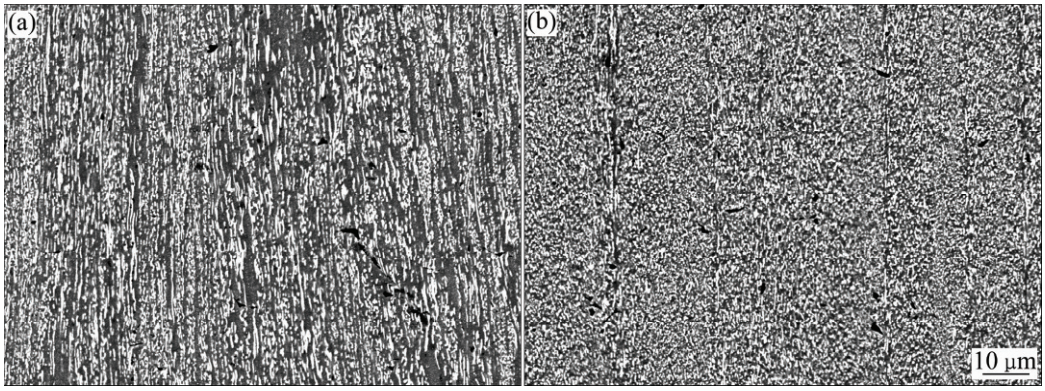

Fig. 3 SEM images of as-rolled $Ti_{42.5}Ni_{42.5}Nb_{15}$ (a) and $Ti_{40}Ni_{40}Nb_{20}$ (b)

For the convenience of comparison, the damping spectrum of as-rolled $Ni_{50}Ti_{50}$ sample is incorporated in the Fig. 4. In fact, the damping spectra records the variation of internal friction with the change of temperature. Since the internal friction is closely associated with the austenite to martensite and martensite to austenite transformations, the characteristic martensitic transformation temperatures and the reverse martensitic transformation temperatures can be distinguished by the spectra. The M_s temperatures as such acquired from the Fig. 4 for as-rolled $(NiTi)_{50-0.5x}Nb_x$ samples are 25, 19.5, 0 and −10 °C, corresponding to the Nb content of 5%, 10%, 15% and 20%, respectively, agreeing with those determined by the curves of electric resistance vs temperature. This is consistent with the conclusion deduced from the XRD patterns as shown in Fig. 1, i.e. the M_s temperatures of $(NiTi)_{50-0.5x}Nb_x$ (x=5, 10, 15) alloys are not far from room temperature. With regard to a few amount of martensite phases detected in $Ti_{45}Ni_{45}Nb_{10}$ with Ms of 19.5 °C and $Ti_{42.5}Ni_{42.5}Nb_{15}$ with

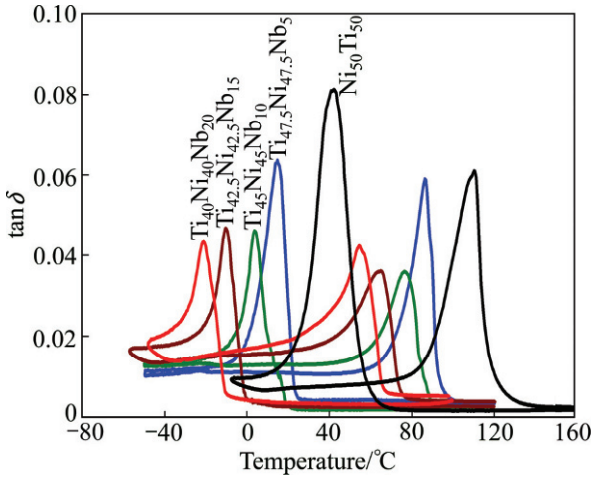

Fig. 4 Damping spectra of as-rolled $(NiTi)_{50-0.5x}Nb_x$ alloy: (a) x=5; (b) x=10; (c) x=15; (d) x=20

M_s of 0 °C, as shown in Fig. 1, this martensite could be attributed to the stress induced martensitic transformation during the sample preparation process.

It has been well known that thermoelastic martensitic transformation could occur either by quenching or by external stress or strain. This means that in the situation of external stress or strain induced martensitic transformation, the external loading can be dissipated to drive the transformation. Consequently, extraordinary internal friction peak always appears corresponding to the whole phase transformation. As a matter of fact, the large value of $\tan\delta$ achieved upon the phase transformation reflects merely an instantaneous damping capacity, not a stable one. Only the plateau value of $\tan\delta$ of full martensite could be used to measure the internal friction of the sample in martensite state. Owing to the hysteresis of the martensitic transformation, the plateau $\tan\delta$ in full martensite state can be extended from the temperature lower than Mf temperature to As temperature.

Figure 4 indicates that the plateau $\tan\delta$ of $(NiTi)_{50-0.5x}Nb_x$ alloys in martensite state increases with the increasing Nb addition from 0 to 20%. It should be noted that all $(NiTi)_{50-0.5x}Nb_x$ alloys exhibit higher plateau $\tan\delta$ than binary $Ni_{50}Ti_{50}$ when they are in martensite state, although the later performs much higher peak value of $\tan\delta$ than the NiTiNb alloys. This could be discussed on the basis of the microstructures of $(NiTi)_{50-0.5x}Nb_x$ in-situ composites.

In view of the effect of Nb addition on the microstructure of $(NiTi)_{50-0.5x}Nb_x$ alloys shown in Fig. 2, the increasing Nb content could increase the volume fraction of the eutectics consisting of NiTi(Nb) and β-Nb phases, accordingly decrease the volume fraction of NiTi(Nb) phase which could performs thermoelastic martensitic transformation. It seems reasonable to conclude that the eutectics could provide better damping capacity than NiTi(Nb) single phase in their martensite state, although only partial constituent, NiTi(Nb) phase, of the eutectics can perform the thermoelastic martensitic transformation. Considering the microstructural features of the eutectics, the better damping capacity of the eutectics should be related to its fine lamellar structure. The existence of fine lamellar results in a large amount of interfaces between the NiTi(Nb) and β-Nb phases. According to the damping mechanisms, interface could be served as an important source of damping materials to dissipate the internal friction [17].

3.3 Mechanical properties of $(NiTi)_{50-0.5x}Nb_x$ (x=5, 10, 15, 20) alloys

In order to examine the mechanical properties, especially the yield strength of the $(NiTi)_{50-0.5x}Nb_x$ alloys in their martensite state, tensile experiments were carried out at the temperatures of (M_s−15 °C). The yield strength, ultimate tensile strength and the ductility of the samples are listed in Table 1. The stress-strain curves of as-rolled $Ni_{50}Ti_{50}$ and $Ni_{42.5}Ti_{42.5}Nb_{15}$ samples are shown in Fig. 5. It is indicated that under the equivalent Ni to Ti ratio and within the amount of Nb addition of the present study, the yield strength of $(NiTi)_{50-0.5x}Nb_x$ series alloys substantially increased with the increasing Nb content. For example, at the temperature of M_s−15 °C, $Ni_{42.5}Ti_{42.5}Nb_{15}$ possesses a yield strength of 289 MPa, corresponding to 192 MPa for $Ni_{50}Ti_{50}$, as shown in Fig. 5. After the addition of Nb from 5% to 20%, these NiTiNb remain to exhibit a good ductility exceeding 20%.

Table 1 Mechanical properties of $Ni_{50}Ti_{50}$ and $(NiTi)_{50-0.5x}Nb_x$ alloys at (M_s−15 °C)

Alloy	Yield strength/MPa	Tensile strength/MPa	Ductility/ %
$Ni_{50}Ti_{50}$	192	801	32.4
$Ni_{47.5}Ti_{47.5}Nb_5$	182	805	24.7
$Ni_{45}Ti_{45}Nb_{10}$	231	836	26.6
$Ni_{42.5}Ti_{42.5}Nb_{15}$	289	801	21.6
$Ni_{40}Ti_{40}Nb_{20}$	276	753	20.6

3.4 $NiTiNb_{15}$ alloys with high damping and high yield strength

As mentioned above, the addition of Nb in $(NiTi)_{50-0.5x}Nb_x$ alloys could result in a moderate decrement of M_s temperatures. For example, the alloys with 15%Nb and 20%Nb are with M_s of 0 and −10 °C,

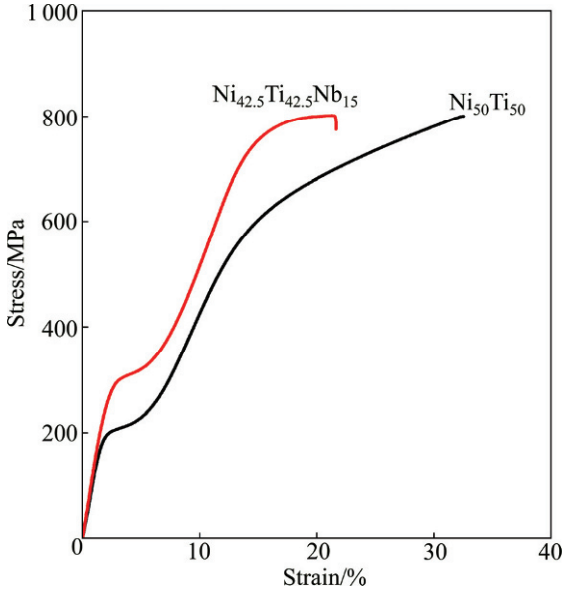

Fig. 5 Stress — strain curves of as-rolled $Ni_{50}Ti_{50}$ and $Ni_{42.5}Ti_{42.5}Nb_{15}$ at (M_s−15 °C)

respectively. Actually, in addition to the high damping capacity and high yield strength, shape memory alloys for high damping engineering application should possess a capability to maintain their high damping capacity in a broad temperature range in which the room temperature is included. This means that it is necessary for these alloys to keep martensite state within a wide temperature range. Considering the hysteresis of martensitic transformation, it is of practical importance to raise the Ms temperature of NiTiNb alloys to or near room temperature. Accordingly, the NiTiNb alloys could perform their high damping capacity at the temperature over the room temperature.

As is well known, Ni/Ti ratio and the content of Nb play key roles in tailoring and controlling the microstructure and the phase transformation behavior of NiTiNb shape memory alloys [2,13,16]. In the present study, a series of $NiTiNb_{15}$ alloys with different Ni/Ti ratios, including $Ni_{43}Ti_{42}Nb_{15}$, $Ni_{42.5}Ti_{42.5}Nb_{15}$, $Ni_{42}Ti_{43}Nb_{15}$ and $Ni_{41}Ti_{44}Nb_{15}$ were prepared, attempting to develop NiTiNb alloys which could demonstrate high damping capacity and high yield strength within a broad temperature range.

The SEM observation of series $NiTiNb_{15}$ alloys indicated that the fraction volumes of primary NiTi(Nb) phase decrease and the fraction volume of eutectics increases with the increasing Ti content from 42% to 44t%. Besides, with the increase of Ti content, more β-Nb phase exist as particles, other than lamellar in the eutectics. Figure 6 plays the SEM images of as-cast $NiTiNb_{15}$ alloys with minimum and maximum content of Ti, $Ni_{43}Ti_{42}Nb_{15}$ and $Ni_{41}Ti_{44}Nb_{15}$, respectively. In Fig. 6,

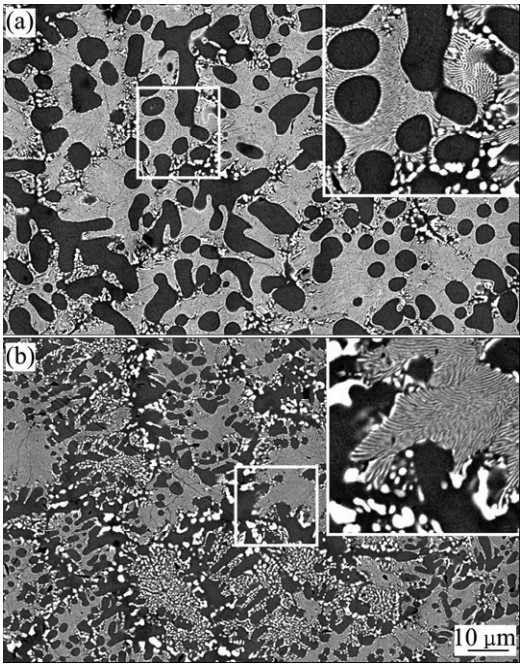

Fig. 6 SEM images of as-cast $Ni_{43}Ti_{42}Nb_{15}$ (a) and $Ni_{41}Ti_{44}Nb_{15}$ (b) as well as corresponding magnifications

the detailed microstructures can be recognized from the magnification of local areas.

Owing to the limitation of the length of the present paper, a systematical investigation will be concentrated on a typical alloy, $Ni_{41}Ti_{44}Nb_{15}$. For the convenience of comparison, Table 2 lists the mechanical properties and the characteristic transformation temperatures M_s and A_s of $Ni_{41}Ti_{44}Nb_{15}$, $Ni_{42.5}Ti_{42.5}Nb_{15}$, and $Ni_{50}Ti_{50}$ shape memory alloys. It is indicated that $Ni_{41}Ti_{44}Nb_{15}$ performs a similar mechanical properties to $Ni_{42.5}Ti_{42.5}Nb_{15}$. The M_s temperature of $Ni_{41}Ti_{44}Nb_{15}$ rises to around room temperature, which is considerably higher than the M_s temperature of for $Ni_{42.5}Ti_{42.5}Nb_{15}$. The M_s temperature of $NiTiNb_5$ alloys increases with increasing ratio of Ti to Ni, with a maximum M_s temperature of 23 °C for $Ni_{41}Ti_{44}Nb_{15}$ alloy. This is in agreement with previous publications [2, 13].

Figure 7 shows the stress-strain curves of as-rolled and as-cast $Ni_{41}Ti_{44}Nb_{15}$ and as-rolled $Ni_{50}Ti_{50}$ alloys at the temperature of 15 °C lower than M_s. The $Ni_{41}Ti_{44}Nb_{15}$

Table 2 M_s and A_s temperatures and mechanical properties of as-rolled $Ni_{50}Ti_{50}$, $Ni_{42.5}Ti_{42.5}Nb_{15}$ and $Ni_{41}Ti_{44}Nb_{15}$ alloys

Alloy	M_s/ °C	A_s/ °C	Yield strength/ MPa	Tensile strength/ MPa	Ductility/ %
$Ni_{42.5}Ti_{42.5}Nb_{15}$	4	40	289	801	21.6
$Ni_{41}Ti_{44}Nb_{15}$	23	56	277	816	47.5
$Ni_{50}Ti_{50}$	58	88	192	801	32.4

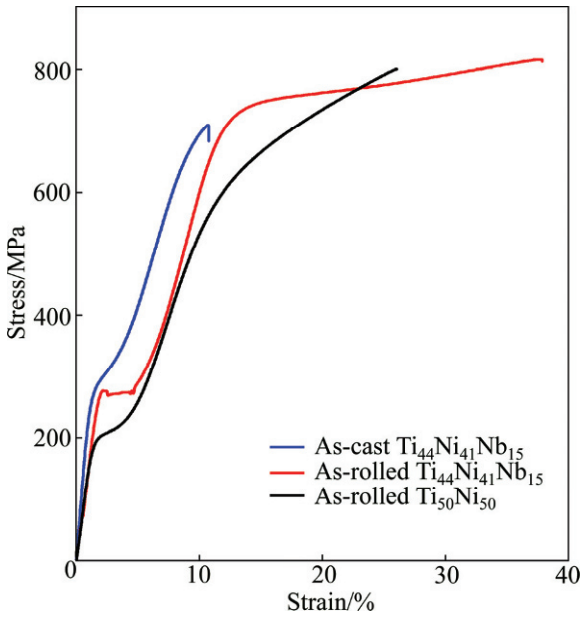

Fig. 7 Stress—strain curves of as-rolled and as-cast $Ni_{41}Ti_{44}Nb_{15}$ and as-rolled $Ni_{50}Ti_{50}$ alloys at temperature of 15 °C lower than M_s

alloy in martensite state demonstrated much higher yield strength for reorientation of martensite than that of binary $Ni_{50}Ti_{50}$, regardless of $Ni_{41}Ti_{44}Nb_{15}$ being as-cast or as-rolled. By comparison of the deformation behaviors of as-cast and as-rolled $Ni_{42.5}Ti_{42.5}Nb_{15}$ alloys shown in Fig. 5, it is found that the deformation of as-rolled $Ni_{41}Ti_{44}Nb_{15}$ proceeds in a Luders-like manner. The reason for this difference is not clear at present. Figure 7 also shows that the hot-rolling treatment can remarkably improve its ductility.

Figure 8 shows the damping spectra of as-rolled $Ni_{50}Ti_{50}$, $Ni_{42.5}Ti_{42.5}Nb_{15}$, $Ni_{42}Ti_{43}Nb_{15}$ and $Ni_{41}Ti_{44}Nb_{15}$ alloys. All the $NiTiNb_{15}$ alloys demonstrated better

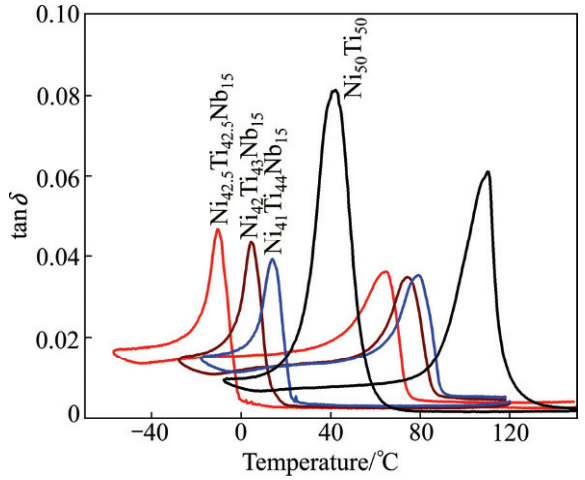

Fig. 8 damping spectra of as-rolled alloys of $Ni_{50}Ti_{50}$, $Ni_{42.5}Ti_{42.5}Nb_{15}$, $Ni_{42}Ti_{43}Nb_{15}$ and $Ni_{41}Ti_{44}Nb_{15}$

damping capacity than binary $Ni_{50}Ti_{50}$ when they are in martensite state. This is in a accordance with the results derived from $(NiTi)_{50-0.5x}Nb_x$ alloys.

By comparison of the damping spectra of NiTiNb and binary $Ni_{50}Ti_{50}$ alloys, one could find an interesting phenomenon. When they are in martensite state, the NiTiNb alloys display substantially higher damping capacity than $Ni_{50}Ti_{50}$. The damping capacity here refers to the plateau tan δ, not the tan δ values located at the peaks originate from the martensitic or reverse martensitic transformations. The reason may be that the tan δ values originating from the transformation are instantaneous, rather than a stable damping capacities. Whereas in austenite state, all the NiTiNb and $Ni_{50}Ti_{50}$ alloys exhibit almost the same damping capacity, although careful analysis could reveals that the TiNiNb austenite performs a slight higher tan δ than that of $Ni_{50}Ti_{50}$.

Above comparison suggests that the eutectic structures or the interfaces play different roles in the improvement of damping capacity, when the NiTiNb alloys are in different states, martensite state or austenite state. Obviously, the interfaces remarkably contribute to improve the damping capacity of NiTiNb alloys in martensite state, but have few contributions to promote their damping capacity when they are in austenite state.

4 Conclusions

1) NiTiNb in-situ composite are composed of primary NiTi(Nb) and fine lamellar eutectics of NiTi(Nb) and β-Nb. Uniform eutectic-like structure could be derived upon a severe deformation. The amount of Nb and the Ni/Ti ratio have remarkable influence on their microstructure, martensitic transformation behavior and mechanical properties of NiTi(Nb) alloys.

2) $Ni_{42.5}Ti_{42.5}Nb_{15}$ and $Ni_{41}Ti_{44}Nb_{15}$ performed much higher damping capacity and yield strength than those of binary $Ni_{50}Ti_{50}$, when the alloys are in their martensite state.

3) Fine eutectic structures provide large amount of interfaces between NiTi(Nb) and β-Nb phases. These interfaces play a key role in the improvement of damping capacity and yield strength of NiTiNb alloys.

References

[1] LAGOUDAS D C. Shape memory alloys, modeling and engineering applications [M]. Springer, 2008.

[2] OTSUKA K, REN X. Physical metallurgy of Ti-Ni-based shape memory alloys [J]. Progress in Materials Science, 2005, 50: 511−678.

[3] DUERIG T W, MELTON K, PROFT J L. Engineering aspects of

shape memory alloys [M]. London: Butterworth-Heinemann, 1990.

[4] LAKES R S. Viscoelastic solids [M]. Boca Raton, USA: CRC Press, 1999.

[5] WANG Y C, LUDWIGSON M, LAKES R S. Deformation of extreme viscoelastic metals and composites [J]. Mater Sci Eng A, 2004, 370: 41−49.

[6] SONG G, MA N, LI H N. Applications of shape memory alloys in civil structures [J]. Engineering Structures, 2006, 28: 1266−1274.

[7] VAN HUMBEECK J. Damping capacity of thermoelastic martensite in shape memory alloys [J]. J Alloys Comp, 2003, 355: 58−64.

[8] AIKEN I D, NIMS K D, WHITTAKER A S, et al. Collapse of the cypress street viaduct as a result of the Loma Prieta earthquake [J]. Earthquake Spectra, 1993, 9(3): 335−370.

[9] GRAESSER E J, COZZARELLI F A. Shape-memory alloys as new materials for aseismic isolation [J]. J Eng Mech, 1991, 117: 2590−2608.

[10] GRAESSER E J. Effect of intrinsic damping on vibration transmissibility of nickel–titanium shape memory alloy springs [J]. Met Mat Trans A, 1995, 26A: 2791−2796.

[11] SHARABASH A M, ANDRAWES B O. Application of shape memory alloy dampers in the seismic control of cable-stayed bridges [J]. Engineering Structures, 2009, 31: 607−616.

[12] ZHAO L C, DUERIG T W, JUSTI S, et al. The study of niobium-rich precipitates in a Ni-Ti-Nb shape memory alloy [J]. Scr Metall, 1990, 24: 221−226.

[13] PIAO M, MIYAZAKI S, OTSUKA K, et al. Effects of Nb addition on the microstructure of Ti-Ni alloys [J]. Mater Trans JIM, 1992, 33: 337−345.

[14] PIAO M, MIYAZAKI, OTSUKA S K. Characteristics of deformation and transformation in $Ni_{47}Ti_{44}Nb_9$ shape memory alloy [J]. Mater Trans JIM, 1992, 33: 346−353.

[15] HE X M, RONG L J, YAN D S, et al. TiNiNb wide hysteresis shape memory alloy with low niobium content [J]. Materials Science and Engineering A, 2004, 371: 193−197.

[16] ZHAO X Q, YAN X M, YANG Y Z, et al. Wide hysteresis NiTi(Nb) shape memory alloys with low Nb content (4.5at%) [J]. Materials Science and Engineering A, 2006, 575: 438−440.

[17] BLANTER M S, GOLOVIN I S, NEUHAUSER H, et al. Internal Friction in Metallic Materials [M]. Springer, 2007.